The Protein Journal
https://doi.org/10.1007/s10930-021-10032-7

Purification and Characterization of Trehalase From *Acyrthosiphon pisum*, a Target for Pest Control

Virgile Neyman[1,2,5] · Frédéric Francis[2] · André Matagne[3] · Marc Dieu[4] · Catherine Michaux[1,6,7] · Eric A. Perpète[1,5,6]

Accepted: 17 November 2021

Abstract

Insect trehalases are glycoside hydrolases essential for trehalose metabolism and stress resistance. We here report the extraction and purification of *Acyrthosiphon pisum* soluble trehalase (ApTreh-1), its biochemical and structural characterization, as well as the determination of its kinetic properties. The protein has been purified by ammonium sulphate precipitation, first followed by an anion-exchange and then by an affinity chromatography. The SDS-PAGE shows a main band at 70 kDa containing two isoforms of ApTreh-1 (X1 and X2), identified by mass spectrometry and slightly contrasting in the C-terminal region. A phylogenetic tree, a multiple sequence alignment, as well as a modelled 3D-structure were constructed and they all reveal the ApTreh-1 similarity to other insect trehalases, *i.e.* the two signature motifs ^{179}PGGRFRELYYWDTY^{192} and ^{479}QWDFPNAWPP^{489}, a glycine-rich region ^{549}GGGGEY^{554}, and the catalytic residues Asp336 and Glu538. The optimum enzyme activity occurs at 45 °C and pH 5.0, with K_m and V_{max} values of ~ 71 mM and ~ 126 µmol/min/mg, respectively. The present structural and functional characterization of soluble *A. pisum* trehalase enters the development of new strategies to control the aphids pest without significant risk for non-target organisms and human health.

Keywords Trehalase · *Acyrthosiphon pisum* · Catalytic and structural properties · Molecular modelling

1 Introduction

Trehalose (α-D-glucopyranosyl-α-D-glucopyranoside) is found in many microorganisms such as bacteria, yeasts [1], plants [2], and invertebrates [3]. In most insects, this non-reducing disaccharide formed by a 1,1-glycosidic bond is known to be the major source of carbohydrate and energy [4]. The hydrolysis of trehalose into two glucose molecules takes place under the enzymatic control of trehalase (Treh) (EC 3.2.1.28). This enzyme was first discovered in *Aspergillus niger* in 1893 [5], and detected in various organisms [1–3, 6–8]. According to the latest classification system of glycoside hydrolases based on their amino acid sequence similarity, Treh is an inverting glycosidase [9] belonging to either of the families 15, 65, and 37. In insects, two distinct Trehs have been characterized so far, both belonging to GH37: a soluble form (Treh-1) found in haemolymph or midgut, and a membrane-bound form (Treh-2) present in flight muscles and follicle cells [3]. Treh-1 activity generally accounts for three-fourths of the total Treh activity ([10]). Whereas some Treh-2 enzymes would be inactive and present in a latent form ([11]). These latter have a putative transmembrane domain near their C-terminus [12]. Both enzymes

Virgile Neyman, Catherine Michaux and Eric A. Perpète have contributed equally to the work.

✉ Catherine Michaux
catherine.michaux@unamur.be

1 Laboratoire de Chimie Physique Des Biomolécules, UCPTS, University of Namur, 61 rue de Bruxelles, 5000 Namur, Belgium

2 Functional and Evolutionary Entomology, TERRA, Gembloux Agro-Bio Tech, University of Liège, 5030 Gembloux, Belgium

3 Laboratoire d'Enzymologie, Centre d'Ingénierie Des Protéines, Institut de Chimie B6, Université de Liège, Sart-Tilman, 4000 Liège, Belgium

4 MaSUN Mass Spectrometry Facility, University of Namur, 61 rue de Bruxelles, 5000 Namur, Belgium

5 Institute of Life Earth and Environment (ILEE), University of Namur, Namur, Belgium

6 Namur Institute of Structures Matter (NISM), University of Namur, Namur, Belgium

7 Namur Research Institute for Life Sciences (NARILIS), University of Namur, Namur, Belgium

Published online: 29 November 2021

have diverse biological roles such as stimulating growth and development, supplying energy for flight, regulating chitin biosynthesis, and recovering from abiotic stress [3].

Whilst the inhibition of chitinase was shown relevant to control harmful insects [13] as it allows for moulting during insect development, Treh only recently received attention as a promising solution for pest control. Indeed, Treh inhibitors such as validamycin A, castanospermine and trehazolin are able to disturb the regulation of trehalose catabolism, causing severe damage such as abnormal development, hampered growth, weight loss, reduced chitin synthesis, decreased flight capacity, lethal metamorphosis, unsuccessful stress recovery, as well as hypoglycaemia [3, 14–16].

Due to their direct action on plants, aphids are major hemipteran pests for forests, cereals, vegetables and fruit crops. Moreover, they are difficult to control due to their high reproductive capability, combined to a short development time. Among them, *Acyrthosiphon pisum* (*A.pisum*), commonly known as the pea aphid, is a sap-sucking insect in the *Aphididae* family. It feeds on several species including legumes and forage crops such as pea, clover, and broad bean. It ranks among the aphid species of major agronomical concern, as it is involved in the transmission of over 40 plant viruses [17]. In addition, the pea aphid is a model organism for biological studies, as its genome has been sequenced and annotated [18].

The reported extractions, purifications and characterizations of insect Trehs usually start from various crude enzyme solutions: blood for *Phormia regina* [6], embryos and larvae for *Artemia* [19], or whole midgut for the silkworm *Bombyx mori* [20] and *Spodoptera frugiperda* [21] and more recently on whole honeybees [22] and whole termites [23]. Gene cloning and prokaryotic expression were also used for Trehs from *Chironomus ramosus* [24], *Drosophila melanogaster* [25] and *Helicoverpa armigera* [8]. In the case of aphids, both soluble and membrane-bound trehalases in apterous and alate morphs of *Aphis citricola* have been observed [26]. More recently, the soluble trehalase of *Aphis glycines* has been described [27], but to the best of our knowledge, no data on *A.pisum* Trehs have been published so far.

Multiple amino acid sequence alignment analysis from bacteria, plants, animals and fungi revealed two Treh signature motifs, *i.e.* -PGGRFXEXYXWDXY- and -QWDXPX[G/A]W[P/A/S]P-, and a glycine rich region (GGGGEY) in the C-terminal region [28, 29]. Gibson et al. [30] have shown that the catalytic domain of *E.coli* trehalase displays an aspartate (Asp312) and a glutamate (Glu496) residues, which respectively play the role of a general acid and a general base, similarly to hydrolases from the GH37 family. By site-directed mutagenesis in *Spodoptera frugiperda*, three arginine residues essential to the enzyme activity were identified inside the active site [28–31]. Up to now, only 10 crystallized structures of Trehs can be found in the Protein Data Bank (PDB): 4 from *E. coli*, 4 from *Saccharomyces cerevisiae,* and 2 from *Enterobacter cloacae*. Like other α-toroidal glycosidases, they show a $(\alpha/\alpha)_6$ barrel fold. No three-dimensional (3D) structure is available from experimental data for Trehs from plants, animals or fungi, whereas molecular modelling studies predict the 3D-structure of insect Trehs in *Helicoverpa armigera* [32], *Bombyx mori* [33], *Drosophila melanogaster* [25], *Tenebrio molitor* [34], *Chironomus riparius* [35], and *Delia antiqua* [36].

The present work is focused on the extraction and purification of the *Acyrthosiphon pisum* soluble trehalase (ApTreh-1) in order to determine its biochemical, structural and kinetic properties. From the amino acid sequence revealed by mass spectrometry, we have built a model 3D-structure. We have also identified the essential amino acids conserved in the vicinity of the active site. To the best of our knowledge, this is the first study reporting the characterization of *A. pisum* Treh.

2 Materials and Methods

2.1 Insects

Aphids were reared in a climate-controlled room (16 h light; 22 ± 1 °C; 70% Relative Humidity). *Acyrthosiphon pisum* Harris, Gembloux clone, were fed for several years on broad bean (*Vicia faba* L., *grosse ordinaire* variety) at Gembloux Agro Bio-Tech, Liège University.

2.2 Materials

HiTrap DEAE-Sepharose Fast Flow, Superdex 200 pg 16/60 and desalting column Sephadex G-25 PD-10 were purchased from GE Healthcare – Life Sciences. The Precision Plus Protein™ Standards Unstained was supplied by Bio-Rad. Other chemicals of analytical grade are from Sigma-Aldrich.

2.3 Enzyme Activity Measurement

Treh activity is determined by the 3,5-dinitrosalicylic acid (DNS) test, a colorimetric assay based on the reduction of DNS in alkaline conditions, which is quantified by absorption spectrophotometry at $\lambda_{max} = 540$ nm [37]. First, 10 µl of the enzyme solution is mixed with 40 µl of 200 mM trehalose and 50 µl of 0.2 M acetate buffer (pH 5), and incubated at 37 °C for 15 min; 300 µl of DNS (10 mg/ml) are then added, and the reaction is stopped in a boiling bath. One unit of enzyme (U) is defined as the enzyme amount that hydrolyses 1 µmol of trehalose per minute. To assess the ApTreh-1 optimal temperature activity, the above-described aliquot was incubated at 4, 25, 37, 45, 50, 55 and 60 °C for 15 min. Similarly, it was incubated for 15 min at 45 °C while

varying pH: 50 mM citric acid-Na_2HPO_4 buffer (pH 3), 0.2 M CH_3COOH/CH_3COONa buffer (pH 4; pH 5), 50 mM NaH_2PO_4/Na_2HPO_4 (pH 6; 7; 8) and 50 mM borate buffer (pH 9). For the kinetics parameters (K_m, V_{max}) determination, increasing concentrations of trehalose (1, 5, 10, 25, 50, 75, 100, 150 and 200 mM) were added and incubated for 15 min at 45 °C and pH 5. Enzyme activity recovery (yield) is determined by:

$$\frac{\text{Total activity from step n}}{\text{Total activity from first step}}.100 \quad (1)$$

where "n" represents the number of purification step.
The purification factor (fold) is obtained by:

$$\frac{\text{Specific activity from step n}}{\text{Specific activity from first step}} \quad (2)$$

where "n" represents the number of purification step.

2.4 Protein Concentration Determination and SDS-PAGE Analysis

Protein content was measured by absorbance at 280 nm with a UV-6300PC spectrophotometer from VWR. For 1-D electrophoresis, proteins and molecular weight standards were loaded on a stacking gel (4% acrylamide, 0.5 M Tris–HCl buffer pH 6.8). Electrophoresis was carried out in a Tris running buffer (0.25 M Tris, 1.9 M glycine, 1% SDS) under 200 V for 1h15. Proteins were then separated in a running gel (12% acrylamide, 1.5 M Tris–HCl buffer pH 8.8). Proteins were stained by the Coomassie Blue staining technic, for which Precision Plus Protein™ Standards Unstained were used as molecular weight standards (ten *Strep*-tagged recombinant proteins: 10, 15, 20, 25, 37, 50, 75, 100, 150, and 250 kDa).

2.5 Mass Spectrometry

The proteins were digested with trypsin following the Filter-Aid Sample Preparation (FASP) protocol [38]. Peptides were analysed by using a nano-LC–ESI–MS/MS maXis Impact UHR-TOF (Bruker, Bremen, Germany) coupled with a nanoLC UltiMate 3000 (Thermo). The digests were separated by reverse-phase liquid chromatography using a 75 µm X 250 mm reverse phase Thermo column (Acclaim PepMap 100 C18) in an Ultimate 3000 liquid chromatography system. Mobile phase A was 95% water/5% acetonitrile with 0.1% formic acid, while mobile phase B was 20% water/80% acetonitrile with 0.1% formic acid. The digest (18 µl) was injected, and the organic content of the mobile phase was linearly increased for 90 min from 5% B to 40% B, and from 40% B to 100% B in 10 more minutes. The column effluent was connected to a Captive Spray (Bruker). Peak lists were created using DataAnalysis 4.2 (Bruker) and searched against the *Aphidoidea* database (from NCBInr) with an automatic decoy database search. Scaffold 4.8 (Proteome Software) was used to validate the MS/MS protein identification based on peptides.

2.6 Amino Acid Sequence Analysis

Isoelectric point, molecular weight and extinction coefficient of ApTreh-1 were estimated by ProtParam tool from ExPASy. The known Trehs sequences from *Aphis glycines*, *Bombyx mori*, *Apis mellifera*, *Tenebrio molitor,* and *Drosophila melanogaster* isoform C were aligned using the T-Coffee multiple sequence alignment followed by BoxShade 3.21. All the conserved regions were compared. For the phylogenetic tree, 38 identified Trehs of various insect orders were obtained from Uniprot, either soluble or membrane-bound forms. The sequences were aligned using the Multiple Sequence Comparison by Log-Expectation (MUSCLE) and were assembled to a neighbour-joining tree using Mega X. For the detection of conserved residues, both Treh isoform sequences from *A.pisum* were aligned using Clustal O 1.2.4 multiple sequence alignment. Putative N-linked glycosylation sites were predicted with NetNGlyc 1.0.

2.7 Homology Modelling and Validation

The 3-D structure prediction of ApTreh-1 was based on a homology modelling method embedded in Swissmodel [39]. With 33% sequence identity, the template was the crystal structure of the periplasmic Treh from *Diamondback moth* gut bacteria, complexed with validoxylamine (PDB ID: 5z66.1, resolution 1.8 Å) [40]. The model was checked for quality and confirmed by Ramachandran plot with MolProbity [41].

2.8 Purification of ApTreh-1

20 g of aphids were ground in a mortar and transferred in 20 ml 0.2 M CH_3COOH/CH_3COONa buffer pH 5. The crude extract, to which the protease inhibitor PMSF (Phenylmethylsulfonyl fluoride) was added, was then placed under constant agitation at 8 °C for 2 h. It was centrifuged at 12,000 g and 4 °C for 30 min, and the supernatant was conserved at 4 °C (S1). In order to extract a maximum amount of enzyme, the pellet was suspended in 10 ml of 0.2 M acetate buffer pH 5, placed again under constant agitation at 8 °C for 2 h, and centrifuged at 12000 g and 4 °C for 30 min. The second supernatant (S2) was stored at 4 °C. S1 and S2 were gathered before fractionation by $(NH_4)_2SO_4$. A first saturation rate of 35% $(NH_4)_2SO_4$ allowed most of the unwanted proteins to precipitate. A second saturation rate of 60% $(NH_4)_2SO_4$ is necessary to obtain a precipitate

containing the Treh. The pellet is solubilized in 5 ml Tris–HCl 20 mM buffer pH 8 and passed through a Sephadex G-25 PD-10 desalting column to eliminate $(NH_4)_2SO_4$ and most of the pigments. The sample was then loaded on a HiTrap™ DEAE-Sepharose Fast Flow column equilibrated with 20 mM Tris–HCl buffer pH 8. Proteins were eluted at 1 ml/min for 30 ml in the same Tris–HCl buffer with a 0 to 1 M NaCl gradient. Trehalase active fractions, identified with the DNS method, were pooled, diluted 10 times in a binding buffer (Tris–HCl pH 7.4; 500 mM NaCl; 1 mM $CaCl_2$; 1 mM $MnCl_2$) and then applied to a HiTrap Con A 4B affinity column equilibrated with the binding buffer. Elution was performed with a Tris–HCl pH 7.4; 500 mM NaCl; 300 mM methyl-α-D-mannoside elution buffer. Trehalase active fractions were finally loaded onto polyacrylamide gel slab (12%) for further investigation.

2.9 Far-UV Circular Dichroism Measurements

The Far-UV circular dichroism (CD) spectrum was recorded with a MOS-500 spectropolarimeter at 20 °C in 20 mM phosphate buffer pH 7, using a 1 mm pathlength quartz Suprasil cell (Hellma), with a protein concentration of ~ 0.1 mg/ml (1.5 µM). Four scans (20 nm/min, 1 nm bandwidth, 0.1 nm data pitch, and 2 s digital integration time) were averaged, base lines were subtracted and no smoothing was applied. Data are presented as the molar residue ellipticity ($[\Theta]_{MRE}$) calculated using the molar concentration of protein and number of residues. Secondary structure analyses using CDSSTR [42, 43], CONTINLL [44, 45] and SELCON3 [43] algorithms were performed on the CD data with the Dichroweb software package [46]. Further analysis was also carried out using the BeStSel algorithm available through the BeStSel server [47]. The results from the four algorithms were averaged and the standard deviations between the calculated secondary structures are given in the results section.

3 Results

3.1 Extraction and Purification of ApTreh-1

ApTreh-1 was extracted and purified from the soluble fraction of a crude aphid extract. The soluble trehalase was isolated after three purification steps using ammonium sulfate precipitation, ion-exchange, and concanavalin columns (Table 1). The enzyme was purified 230-fold, which gives a specific activity of 88.6 µmol/min/mg. Approximately 0.3 mg of ApTreh1 was recovered from 20 g of aphids, in line with the extraction-purification yield observed for Treh in *Artemia* embryos and larvae [19].

The crude extract of aphids was first suspended in a pH 5 buffer, as it was found optimal for the extraction step (Fig S1). The $(NH_4)_2SO_4$ precipitation, allowed for a fivefold purification and for removing irrelevant proteins, while maintaining high specific activity. More importantly, this step eliminates the pigments present in *A.pisum* (typically aphins and carotenoids) [48, 49], which can cause severe damage to the chromatographic columns. The sample was then applied on a HiTrap DEAE-Sepharose Fast Flow (FPLC system) with a linear increasing gradient in NaCl concentration. Treh active fractions were pooled, showing a eightfold purification and a 60% of activity recovery. They were finally run on a HiTrap Con 4B, and Treh active fractions were loaded on a SDS-PAGE gel (12%). The enzyme was detected with the Coomassie blue G-250 staining and showed a major protein band at about 70 kDa (Fig. 1).

3.2 Sequence and Phylogenetic Analysis

The 70 kDa band observed on SDS-PAGE has been analysed by mass spectrometry (MS). From the MS identified peptides (Fig S4 – Table S2) and the *A. pisum* Trehs sequence predicted in the Uniprot database, two isoforms (X1 and X2) were revealed (Fig. 2). They are actually encoded by the same gene (gene ID from GenBank: 100,161,043), and most probably the result of an alternative splicing on the last coding exon. Indeed, X1 is 17 amino-acids longer compared to X2, and X2 differs from X1 by only 6 amino acids in the C-terminal end. On the basis of their respective amino acid

Table 1 Summary of the purification steps of ApTreh-1

Procedure	Total activity (U or µmol/min)	Total protein (mg)	Specific activity (U/mg)	Yield (%)	Purification factor (fold)
Crude extract	253.4	660.2	0.4	100	1.0
Ammonium sulfate precipitation	214.3	103.1	2.1	85	5
DEAE-Sepharose	151.3	52.3	2.9	60	8
Concanavaline A 4B	26.4	0.3	88.6	10	231

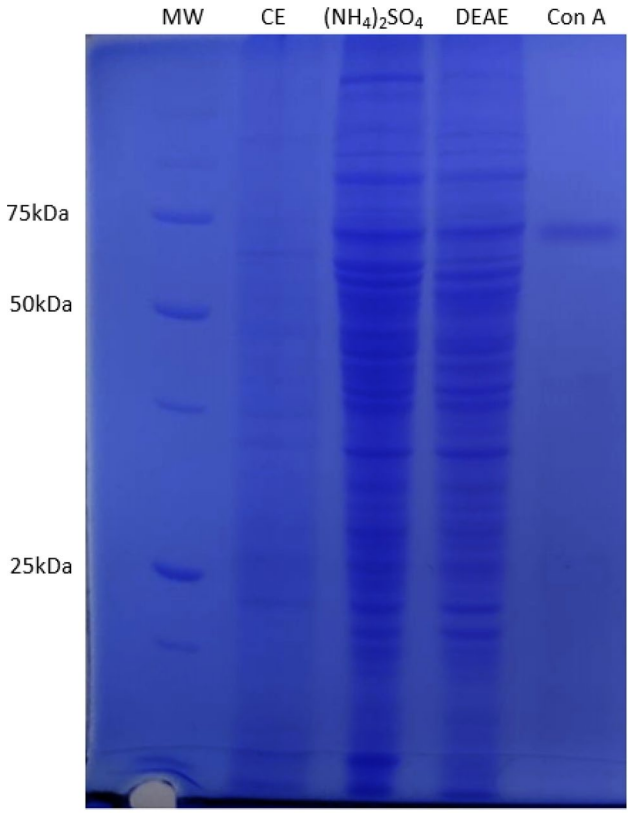

Fig. 1 1-D SDS-PAGE 12% polyacrylamide handmade gels with every purification steps: *CE* Crude Extract, *$(NH_4)_2SO_4$* Ammonium sulphate precipitation, *DEAE* Anion Exchange Chromatography, *Con A* Affinity Chromatography

sequence, we calculated their molecular weights and isoelectric points: 70,400 Da and 6.3 for isoform X1, and 68,300 and 6.2 for isoform X2.

MS analysis also shown that the isoform X2 was the most abundant protein in the sample and peptides detected represents 46% of coverage (based on the complete sequence containing signal peptide) on the entire protein sequence. This enzyme was therefore chosen for the further analyses.

Multiple amino acid sequence alignment of ApTreh-1 (isoform X2; J9JPV2 on Uniprot) and other Trehs from various insect orders (*Aphis glycines*, *Bombyx mori*, *Apis mellifera*, *Tenebrio molitor,* and *Drosophila melanogaster*) shows that ApTreh-1 shares a significant sequence similarity (40–81% identity) with the other Trehs (Table S1). As *Aphis glycines* and *Acyrthosiphon pisum* belong to the same order and family, they share a higher sequence identity percentage than other species. ApTreh-1 contains the two Treh signature motifs [29] (^{179}PGGRFRELYYWDTY^{192} and ^{479}QWDFPNAWPP^{489}), a glycine-rich region (^{549}GGGGEY^{554}) highly conserved among the species, as well as the catalytic residues Asp336 and Glu538 which are typical of the GH37 hydrolase family [30] (Fig. 3). In addition from the PFAM database, ApTreh-1 is found to belong to the six-hairpin glycosidase superfamily. The success of the Concanavalin A affinity purification is indeed an indication of substantial glycosylation of the protein. Residues 234, 346, 424 and 481 were detected to be four potential N-linked glycosylation sites.

The phylogenetic tree based on amino acid sequences of Trehs from various insect species unsurprisingly presents two branches separating both types of Treh (Treh-1 and Treh-2) (Fig. 4). As expected, ApTreh-1 is very close to those from other aphids. Noteworthily, it is grouped with other well-known pests hemiptera, such as sweetpotato whitefly (*Bemisia tabaci*), small brown planthopper (*Laodelphax striatellus*), and brown planthopper (*Nilaparvata lugens*).

3.3 Structure of ApTreh-1

The secondary structure of ApTreh-1 was characterized by CD (Fig. 5). The spectrum is typical of a protein with a relatively high content in α-helical structure. Calculation of the secondary structure content of the enzyme gives the following values: 33 ± 3% α-helices, 17.2 ± 0.8% β-strands, 18 ± 4% turns and 32 ± 5% unordered.

As the PDB databank misses 3-D structure of any animal trehalase, we have selected homology modelling to build a structural model for ApTreh-1. The crystal structure of periplasmic Treh from Diamondback moth gut bacteria complexed with validoxylamine (PDB ID: 5z66, 1.8 Å) has been selected as template. The ApTreh-1 shows a 33% sequence identity and 84% sequence coverage with the template. The validity of the model is supported by a Ramachandran plot showing 92% of the residues lying in the allowed regions (Fig.S3). The trehalase central catalytic $(\alpha/\alpha)_6$ barrel fold being exclusively composed of 12 α-helices (Fig. 6A), most of the residues are in the Ramachandran α-helix region. In addition, the model is in agreement (39.2% α-helix and 10.4% β-strands) with the CD data.

The ApTreh-1 model has a 0.2 Å alpha-carbon root-mean-square deviation from the template. It shares the same fold with that from periplasmic Treh of *Diamondback moth* gut bacteria (Fig.S2). 24 amino acids are identified within 5 Å of validoxylamine, 9 of them being aromatics (F183, Y187, W189, Y232, W335, W486, W492, Y554, W562). This part of the active site is conserved between *A. pisum* and the *Diamondback moth* gut bacteria. By analogy with the template structure, we have identified Asp336 and Glu538 as putative acid and base catalytic residues, together with three essential arginine residues [31]: Arg182, Arg235 and Arg300 (Fig. 6). In most insects trehalases, the glycine-rich region is part of a mobile "lid loop" identified as playing an important role in substrate and inhibitor recognition [40]. In ApTreh-1, this corresponds to the sequence

Fig. 2 Amino acid sequence alignment of the two ApTreh-1 isoforms identified by LC-MSMS method. The sequences used in the alignment are: Isoform X1 (XP_003245895.1 on NCBI) and isoform X2 (XP_001950264.1 on NCBI). The red line corresponds to the sequence part in the C-terminal region that differs between the isoforms (Color figure online)

^{548}TGGGGEYTPQTGF^{561} (Fig. 6). Similar flexible glycine-rich loops are also observed in other glycosidases such as amylases [50]. This loop is in close contact with crucial residues of the active site, and the following interactions allow for the closure of the lid loop towards the active site: i) the electrostatic interaction between Glu553 and Arg300, ii) the CH…π interaction between Tyr554 and Phe183, iii) the cation-π interaction between Tyr554 and Arg182, and iv) the H-bond between Tyr554 and the catalytic residues Asp336/538 (depending on the position of the hydrogen of the Tyr554 OH- group).

Another region, called "hood-like domain" in Treh of Diamondback moth gut bacteria, is also present in ApTreh-1 from ^{44}Q to ^{100} M (Fig. 6). It is hypothesized to close the catalytic pocket after ligand binding [40]. The moderately conserved (Fig. 3) ^{65}DSKTFV^{70} region closely interacts with the active site as Asp65 and Lys67 electrostatically interact with Arg182 and Glu185, respectively. Moreover, an H-bond is observed between Ser66 and Glu306 (Fig. 7).

3.4 Catalytic and Kinetics Properties of the Enzyme

For catalytic and kinetics studies, trehalose was used for substrate as its specificity for trehalases has previously been assessed for insect trehalases [51]. The effect of temperature and pH on the Treh activity is first investigated, and we

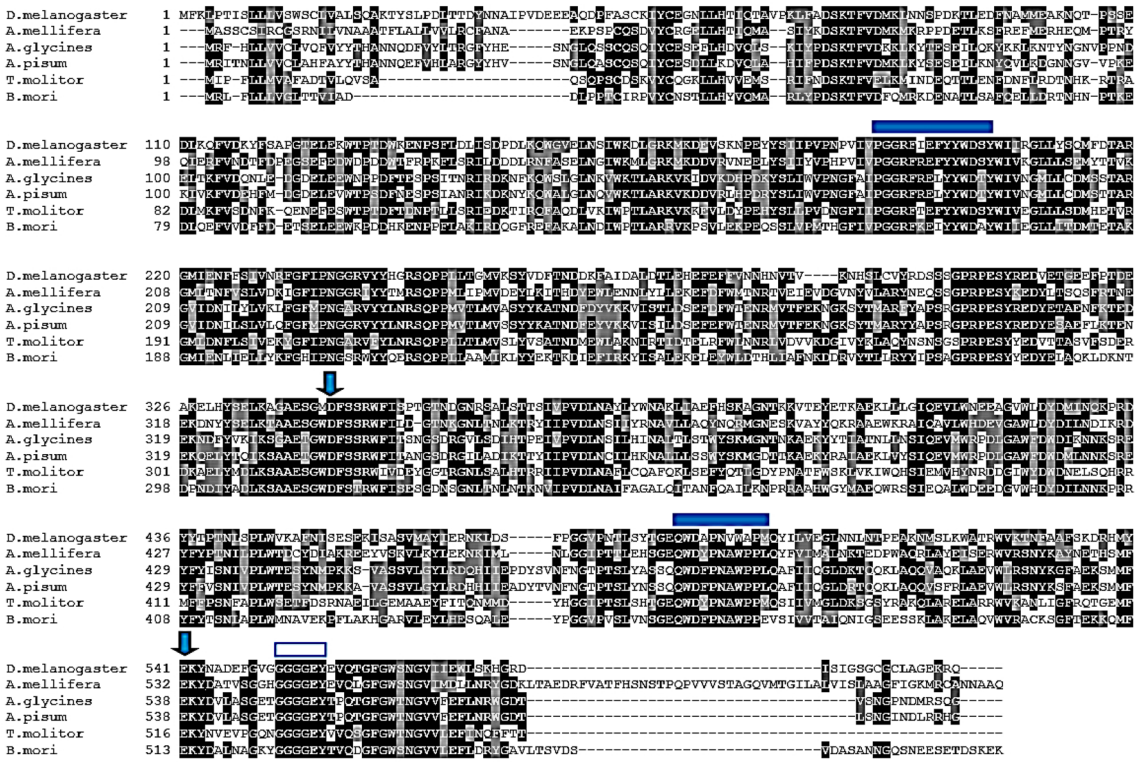

Fig. 3 Multiple amino acid sequence alignment of soluble Trehs from *Acyrthosiphon pisum* (Isoform X2, J9JPV2 on Uniprot), *Aphis glycines* (I1YDC3), *Tenebrio molitor* (P32359), *Bombyx mori* (P32358), *Apis mellifera* (A8J4S9) and *Drosophila melanogaster* (Q9W2M2). Full blue boxes represent signature motifs in Trehs; the empty blue box is the glycine-rich region; and blue arrows are the catalytic residues (Color figure online)

have determined an optimal enzyme temperature of 45 °C (Fig. 8A). Generally for insects trehalase, the optimum temperature lies between 45 and 65 °C [3]. We observe a 71% reduction of Treh activity at 55 °C, while at 60 °C it is reduced by 86%. We conclude that unlike some insect Trehs having shown thermostability [25], ApTreh-1 is not a heat-resistant enzyme.

The maximum hydrolysis rate is obtained in a 0.2 M sodium acetate buffer, pH 5 (Fig. 8B) in line with the 5-to-7 pH range generally reported for insect trehalases [3]. As the tris(hydroxymethyl)aminomethane was previously described as a Treh inhibitor [3], it has been cautiously avoided as buffer in the present study. Furthermore, we have observed that ApTreh-1 loses its enzymatic activity in alkaline ($pH > 9$) or in extreme acidic conditions ($pH < 2$).

The kinetic parameters (K_m and V_{max}) of ApTreh-1 were investigated at optimum pH 5 and temperature = 45 °C. Using a substrate concentration varying from 1 to 200 mM, the enzyme presents a typical Michaelis–Menten plot (Fig. 9A), and the Hanes-Woolf model adequately describes the enzyme activity with $R^2 = 0.96$ (Fig. 9B). The K_m and V_{max} values are 71 mM and 126 µmol/min/mg, respectively. k_{cat} is evaluated at 143 s^{-1}, and k_{cat}/K_m is 2 $mM^{-1}.s^{-1}$. This is in agreement with the K_m values ranging from 0.5 to 73 mM that have been reported from other insects trehalases, such as *Apis mellifera* (0.52 mM) [52], *Artemia* Embryos (8.4 mM) [19], *Bombyx mori* (0.46 mM) [20], *Aphis citricola* (6.4 mM from alate – 7.2 mM from apterous) [26], *Chaetomium aureum* (0.7 mM) [53] and *Helicoverpa armigera* (72.8 mM)[8].

4 Discussion

This study reports the first isolation and three-step purification (ammonium sulphate precipitation, anion-exchange, and concanavalin chromatography) of the pea aphid (Acyrthosiphon pisum) soluble trehalase. Aphids are major pests that feed on phloem sap, weakening the plant and causing a metabolic imbalance, while also introducing toxins in plants. As the currently used insecticides are gradually less effective against these harmful insects, alternatives are urgently needed. As targeting aphid trehalases seems a promising solution, characterizing these enzymes is a crucial step.

Using/by means of mass spectrometry analysis, we have identified for the first time two isoforms of ApTreh-1, with a molecular weight of 70.4 kDa for isoform X1, and 68.3 kDa for isoform X2, which only differ by their

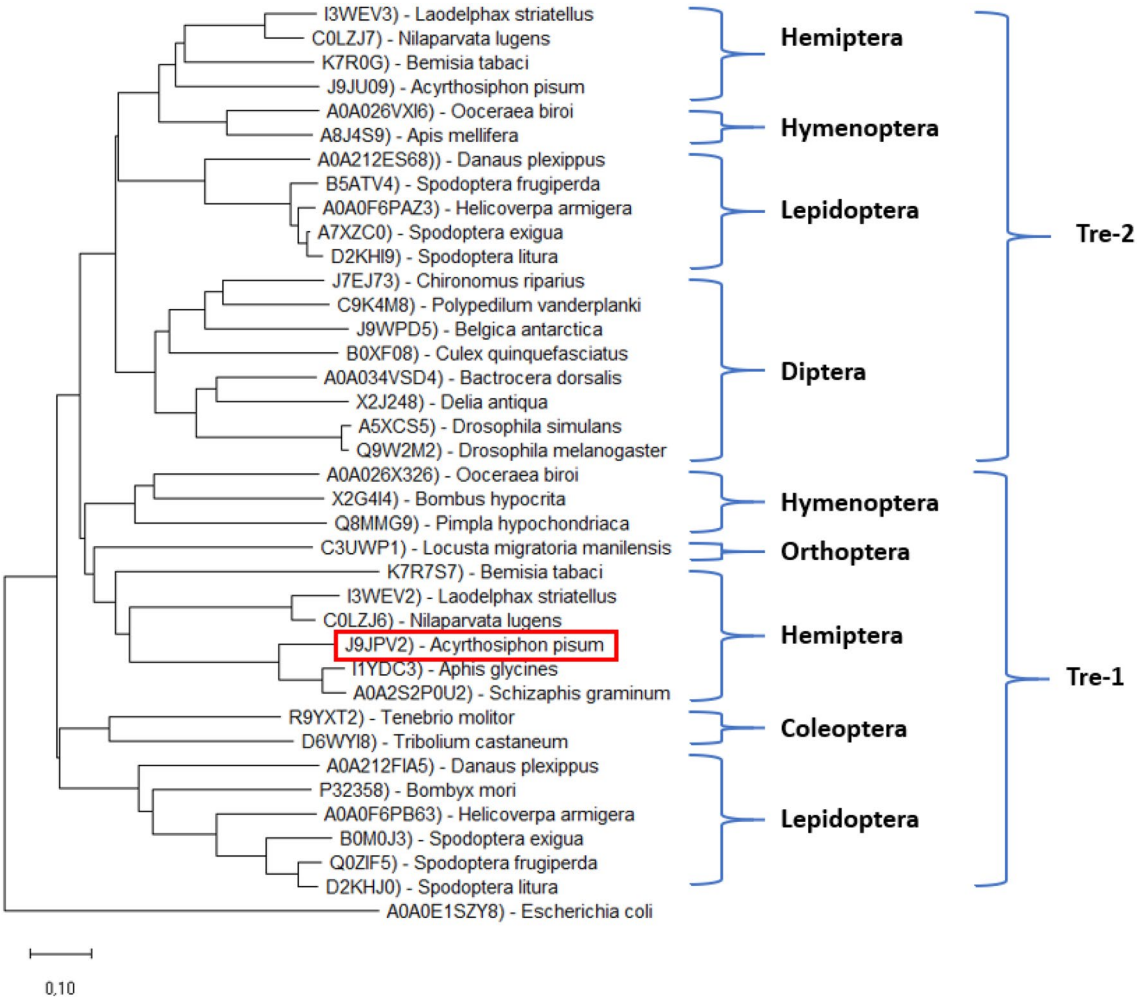

Fig. 4 Phylogenetic analysis of insect Trehs across different insect species. Treh sequences were obtained from the Uniprot database and aligned using MUSCLE

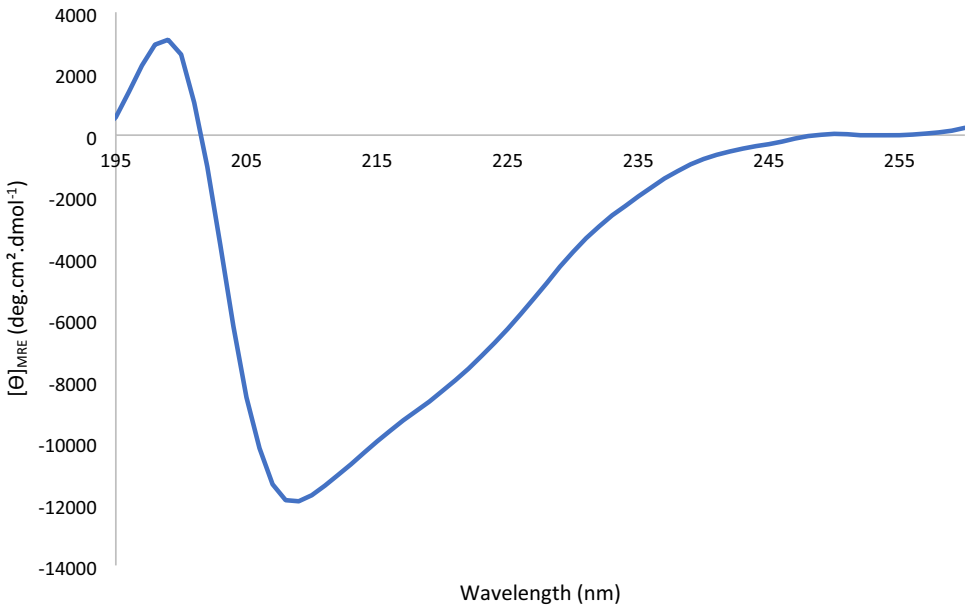

Fig. 5 Far-UV CD spectrum of ApTreh-1**.** Data were obtained at 20 °C, in 20 mM phosphate buffer pH 7. The protein concentration was 1.5 µM. Helical content is ~ 33% (see text for further details)

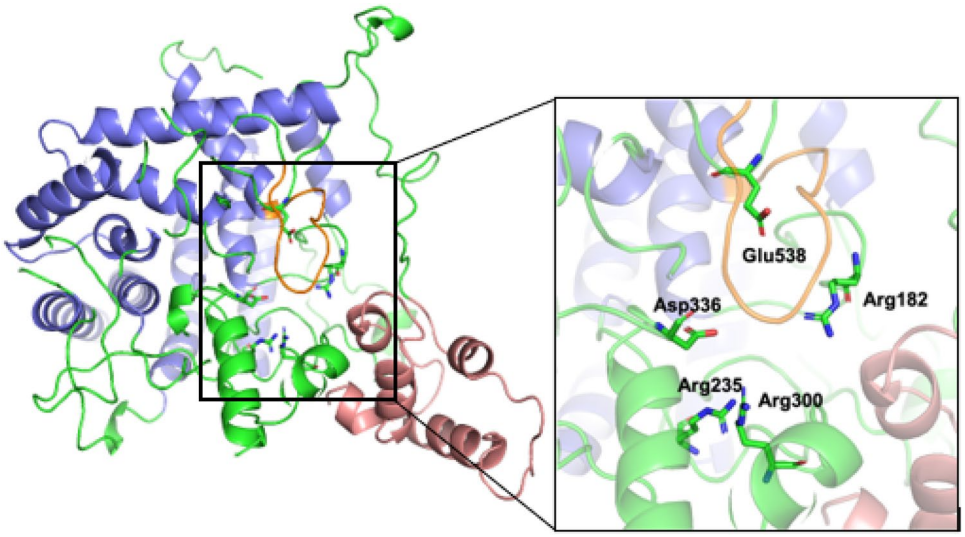

Fig. 6 The ApTreh-1 model. The 12 α-helices of the central catalytic $(\alpha/\alpha)_6$ barrel fold are coloured in blue. The two catalytic residues and three arginines residues are represented in sticks; the lid loop and the hood-like domain are pictured in orange and rose, respectively (Color figure online)

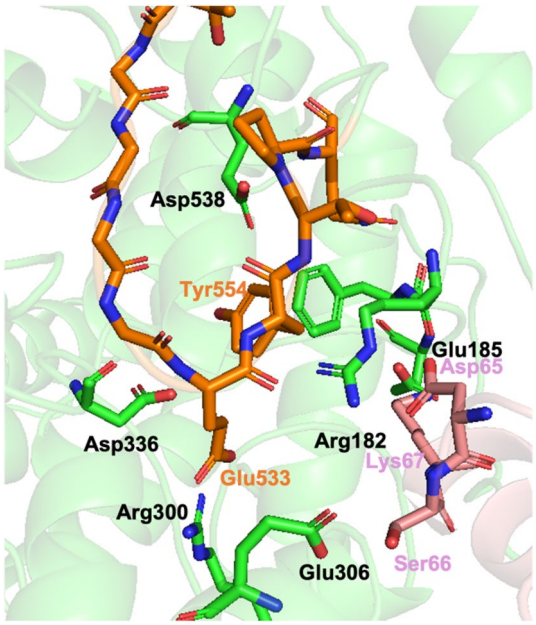

Fig. 7 The lid loop (in orange) and the hood-like domain (in rose) in interaction with the catalytic site of ApTreh-1 (Color figure online)

C-terminal end amino acids. Other cases of soluble trehalase isoforms were discovered in insects such as *Drosophila melanogaster* (DmTrehA, B and C) [25], *Harmonia axyridis* (HaTreh1-1, HaTreh1-2, HaTreh1-3, HaTreh1-4, HaTreh1-5) [54, 55] or *Tribolium castaneum* (TcTre1-1, TcTre1-2, TcTre1-3, TcTre1-4) [56]. It is worth mentioning that similarly to Hemipterans such as *Diaphorina citri* (DcTre1-1, DcTre1-2) [57] and *Nilaparvata lugens* (NlTre1-1, NlTre1-2) [58], two soluble trehalases have also been identified in *Acyrthosiphon pisum*. These studies highlighted specific functions of these isoforms, either in chitin biosynthesis or in regulation towards a hot or cold environment. In addition, a recent genomic and phylogenetic analysis showed that trehalase genes have been more frequently duplicated in Hemipterans than in other insects [59]. Understanding the specific biochemical and physiological roles of these two isoforms is therefore pertinent from an evolutionary point of view.

Treh-1 was catalytically and kinetically characterized and we were able to point out an optimal enzyme temperature and pH of 45 °C and 5, respectively. These data allows for future comparisons with other insect trehalases and for inhibition studies.

Finally, a model of the 3D-structure of ApTreh-1 was built by homology modelling and supported by geometrical criteria as well as by CD measurements. The active site containing two catalytic residues (Asp336 and Glu538) and three arginine essential for the activity was located by multiple sequence alignment with other insect trehalases. A glycine-rich mobile "lid loop" and a "hood-like domain" were also identified, whose flexibility has been hypothesized to play a crucial role in inhibitor binding. Forthcoming modelling studies aiming to design ApTreh-1 inhibitors will take these structural features into account. Furthermore, all the analyses performed in the present work will focus on/explore the A. pisum membrane-bound Treh in order to better understand the specific implications of each of these enzymes. This crucial information will further help design aphid trehalase inhibitors.

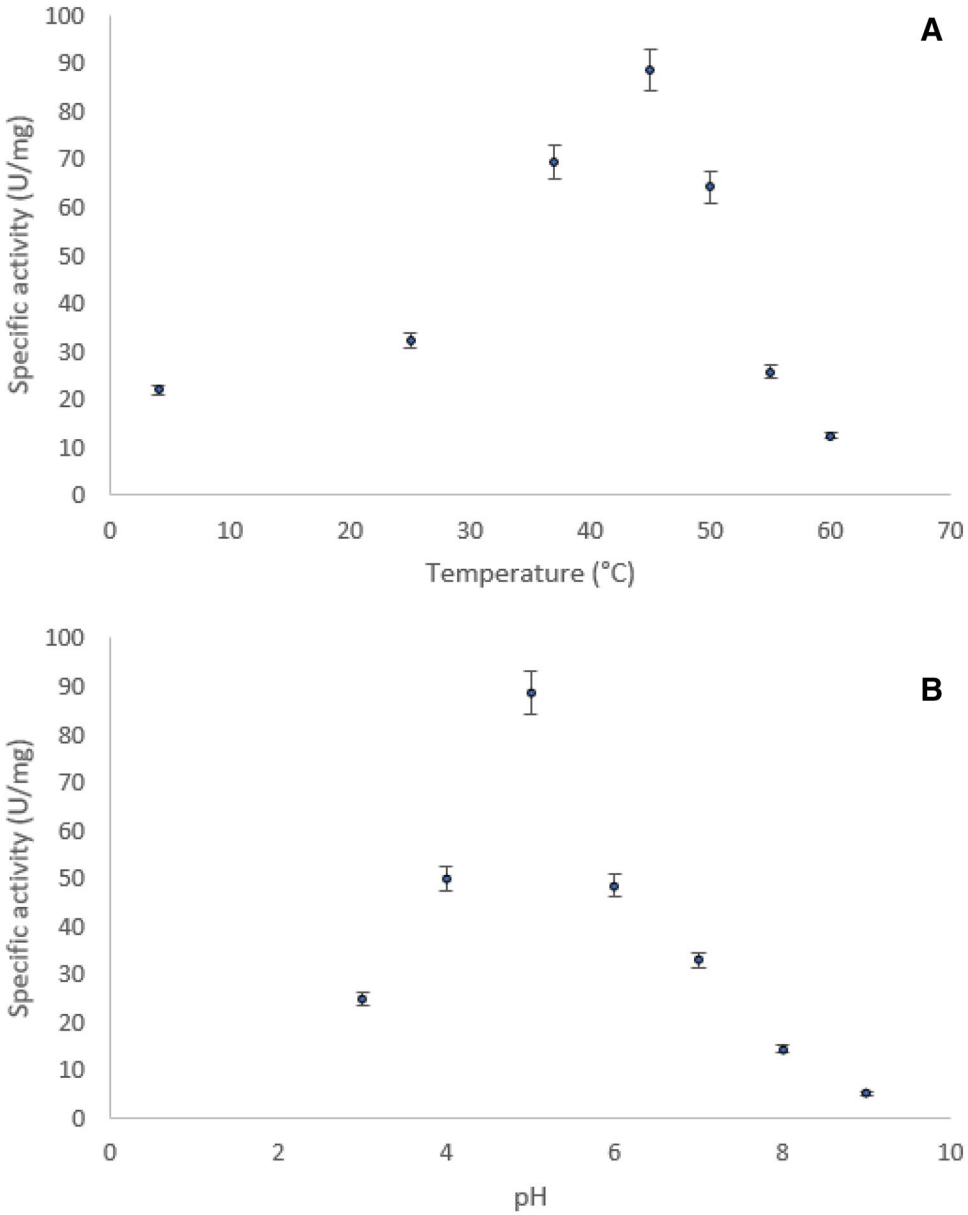

Fig. 8 Effect of **A** temperature and **B** pH on the activity of ApTre-1. The sample were analyzed in triplicate

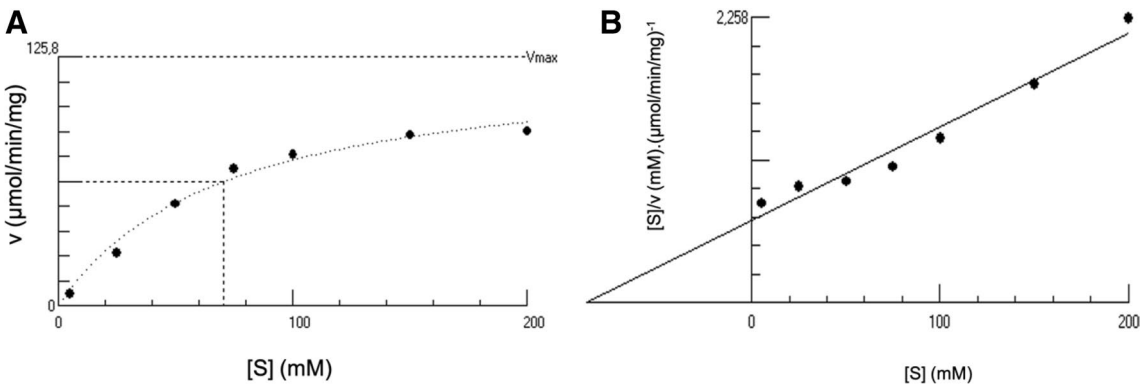

Fig. 9 **A** Michaelis–Menten and**B** Hanes-Woolf plot of ApTreh-1, with concentration of trehalose varying from 1 to 200 mM. Hyper32 program has been used to obtain both plots

Acknowledgements This work was supported by the Win^{2}Wal research program -Exercise 2019 (convention n°1910079). This research used resources of the "Platforme Technologique de Calcul Intensif (PTCI)" and "Plateforme Technologique de Spectrométrie de Masse (MaSUN)", located at the University of Namur, Belgium. Catherine Michaux and Eric A. Perpète thank the Belgian National Fund for Scientific Research for their respective associate and senior research associate positions.

Author Contributions Conception of the work: CM, EAP, FF. Collection and analysis of data: CM, EAP, VN, MD, AM. Writing manuscript: CM, EAP, VN.

Data Availability The datasets generated during and/or analysed during the current study are available from the corresponding author on reasonable request.

References

1. Horlacher R, Uhland K, Klein W et al (1996) Characterization of a cytoplasmic trehalase of *Escherichia coli*. J Bacteriol 178:6250–6257. https://doi.org/10.1128/jb.178.21.6250-6257.1996
2. Müller J, Boller T, Wiemken A (1995) Trehalose and trehalase in plants: recent developments. Plant Sci 112:1–9. https://doi.org/10.1016/0168-9452(95)04218-J
3. Shukla E, Thorat LJ, Nath BB, Gaikwad SM (2015) Insect trehalase: Physiological significance and potential applications. Glycobiology 25:357–367. https://doi.org/10.1093/glycob/cwu125
4. Thompson SN (2003) Trehalose—the insect "Blood" Sugar. Advances in Insect Physiology 31(03):205–285
5. Bourquelot E (1893) Transformation du trehalose en glucose dans les champignons par un ferment soluble : la trehalase. Bull la Société Mycol Fr 9:189–194
6. Friedman S (1960) Purification and properties of trehalase isolated from Phormia Regina, Meig. Archives of Biochemistry and Biophysics 87(2):252–258
7. Lucia A, Zimmermann S, Terenzi F, Jorge JA (1990) Purification and properties of an extracellular conidial trehalase from Humicola grisea var.thermoidea. Biochim Biophys Acta 1036:41–46
8. Ai D, Cheng S, Chang H et al (2018) Gene cloning, prokaryotic expression, and biochemical characterization of a soluble trehalase in helicoverpa armigera hübner (Lepidoptera: Noctuidae). J Insect Sci 18:2–9. https://doi.org/10.1093/jisesa/iey056
9. Davies G, Henrissat B (1995) Structures and mechanisms of glycosyl hydrolases. Structure 3:853–859. https://doi.org/10.1016/S0969-2126(01)00220-9
10. Tatun N, Singtripop T, Tungjitwitayakul J, Sakurai S (2008) Regulation of soluble and membrane-bound trehalase activity and expression of the enzyme in the larval midgut of the bamboo borer Omphisa fuscidentalis. Insect Biochem Mol Biol 38:788–795. https://doi.org/10.1016/j.ibmb.2008.05.003
11. Wegener G, Tschiedel V, Schlöder P, Ando O (2003) The toxic and lethal effects of the trehalase inhibitor trehazolin in locusts are caused by hypoglycaemia. J Exp Biol 206:1233–1240. https://doi.org/10.1242/jeb.00217
12. Tang B, Chen X, Liu Y et al (2008) Characterization and expression patterns of a membrane-bound trehalase from Spodoptera exigua. BMC Mol Biol 9:1–12. https://doi.org/10.1186/1471-2199-9-51
13. Francis F, Saguez J, Cherqui A et al (2012) Purification and characterisation of a 31-kDa chitinase from the Myzus Persicae aphid: A target for hemiptera biocontrol. Appl Biochem Biotechnol 166:1291–1300. https://doi.org/10.1007/s12010-011-9517-3
14. Tatun N, Tungjitwitayakul J, Sakurai S (2016) Developmental and lethal effects of trehalase inhibitor (Validamycin) on the Tribolium castaneum (Coleoptera: Tenebrionidae). Ann Entomol Soc Am 109:224–231. https://doi.org/10.1093/aesa/sav111
15. El Nemr A, El Ashry ESH (2011) Potential trehalase inhibitors. Syntheses of trehazolin and its analogues, 1st edn. Elsevier, Amsterdam, pp 45–114
16. Asano N, Takeuchi M, Kameda Y et al (1990) Trehalase inhibitors, validoxylamine A and related compounds as insecticides. J Antibiot (Tokyo) 43:722–726
17. Sylvester ES (1980) Circulative and propagative virus transmission by aphids. Annu Rev Entomol 25:257–286
18. Richards S, Gibbs RA, Gerardo NM et al (2010) Genome sequence of the pea aphid Acyrthosiphon pisum. PLoS Biol. https://doi.org/10.1371/journal.pbio.1000313
19. Nambu Z, Nambu F, Tanaka S (1997) Purification and characterization of Trehalose from Artemia embryos and larvae. Zoolog Sci 14:419–427
20. Sumida M, Yamashitat O (1983) Purification and some properties of soluble trehalase from midgut of pharate adult of the silkworm. Bombyx mori 13:257–265
21. Silva MCP, Terra WR, Ferreira C (2004) The role of carboxyl, guanidine and imidazole groups in catalysis by a midgut trehalase purified from an insect larvae. Insect Biochem Mol Biol 34:1089–1099. https://doi.org/10.1016/j.ibmb.2004.07.001
22. Lee JH, Tsuji M, Nakamura M et al (2001) Purification and identification of the essential ionizable groups of honeybee, Apis mellifera L., trehalase. Biosci Biotechnol Biochem 65:2657–2665. https://doi.org/10.1271/bbb.65.2657
23. Jin LQ, Zheng YG (2009) Inhibitory effects of validamycin compounds on the termites trehalase. Pestic Biochem Physiol 95:28–32. https://doi.org/10.1016/j.pestbp.2009.05.001
24. Shukla E, Thorat L, Bendre AD et al (2018) Cloning and characterization of trehalase: a conserved glycosidase from oriental midge Chironomus ramosus. 3 Biotech. https://doi.org/10.1007/s13205-018-1376-y
25. Shukla E, Thorat L, Bhavnani V et al (2016) Molecular cloning and in silico studies of physiologically significant trehalase from Drosophila melanogaster. Int J Biol Macromol 92:282–292. https://doi.org/10.1016/j.ijbiomac.2016.06.097
26. Neubauer I, Ishaaya I, Aharonson N, Raccah B (1980) Activity of soluble and membrane-bound threhalase in apterous and alate morphs of Aphis citricola. Comp Biochem Physiol B Biochem 66:505–510. https://doi.org/10.1016/0305-0491(80)90240-0
27. Bansal R, Mian MAR, Mittapalli O, Michel AP (2013) Molecular characterization and expression analysis of soluble trehalase gene in Aphis glycines, a migratory pest of soybean. Bull Entomol Res 103:286–295. https://doi.org/10.1017/S0007485312000697
28. Silva MCP, Terra WR, Ferreira C (2010) The catalytic and other residues essential for the activity of the midgut trehalase from Spodoptera frugiperda. Insect Biochem Mol Biol 40:733–741. https://doi.org/10.1016/j.ibmb.2010.07.006
29. Barraza A, Sánchez F (2013) Trehalases: A neglected carbon metabolism regulator? Plant Signal Behav 8:1–5. https://doi.org/10.4161/psb.24778
30. Gibson RP, Gloster TM, Roberts S et al (2007) Molecular basis for Trehalose inhibition revealed by the structure of Trehalose in complex with potent inhibitors. Angew Chemie 119:4193–4197. https://doi.org/10.1002/ange.200604825
31. Terra WR, Barroso IG, Dias RO, Ferreira C (2019) Molecular physiology of insect midgut, 1st edn. Elsevier, Amsterdam, pp 117–163

32. Ai D, Lin R, Wang M et al (2018) Chemical modification of soluble trehalase from Helicoverpa armigera (Lepidoptera:Noctuiadae). Acta Entomol Sin 61:801–807
33. Zhou Y, Li X, Katsuma S et al (2019) Duplication and diversification of trehalase confers evolutionary advantages on lepidopteran insects. Mol Ecol 28:5282–5298. https://doi.org/10.1111/mec.15291
34. Gomez A, Cardoso C, Genta FA et al (2013) Active site characterization and molecular cloning of Tenebrio molitor midgut trehalase and comments on their insect homologs. Insect Biochem Mol Biol 43:768–780. https://doi.org/10.1016/j.ibmb.2013.05.010
35. Forcella M, Mozzi A, Bigi A et al (2012) Molecular cloning of soluble trehalase from chironomus riparius larvae, its heterologous expression in escherichia coli and bioinformatic analysis. Arch Insect Biochem Physiol 81:77–89. https://doi.org/10.1002/arch.21041
36. Guo Q, Hao YJ, Li Y et al (2015) Gene cloning, characterization and expression and enzymatic activities related to trehalose metabolism during diapause of the onion maggot Delia antiqua (Diptera: Anthomyiidae). Gene 565:106–115. https://doi.org/10.1016/j.gene.2015.03.070
37. Lindsay H (1973) A colorimetric estimation of reducing sugars in potatoes with 3,5-dinitrosalicylic acid. Potato Res 16:176–179. https://doi.org/10.1007/BF02356048
38. Distler U, Kuharev J, Navarro P, Tenzer S (2016) Label-free quantification in ion mobility-enhanced data-independent acquisition proteomics. Nat Protoc 11:795–812. https://doi.org/10.1038/nprot.2016.042
39. Waterhouse A, Bertoni M, Bienert S et al (2018) SWISS-MODEL: Homology modelling of protein structures and complexes. Nucleic Acids Res 46:296–303. https://doi.org/10.1093/nar/gky427
40. Adhav A, Harne S, Bhide A et al (2019) Mechanistic insights into enzymatic catalysis by trehalase from the insect gut endosymbiont Enterobacter cloacae. FEBS J 286:1700–1716. https://doi.org/10.1111/febs.14760
41. Davis IW, Leaver-Fay A, Chen VB et al (2007) MolProbity: All-atom contacts and structure validation for proteins and nucleic acids. Nucleic Acids Res 35:375–383. https://doi.org/10.1093/nar/gkm216
42. Manavalan P, Johnson WC (1987) Variable selection method improves the prediction of protein secondary structure from circular dichroism spectra. Anal Biochem 167:76–85. https://doi.org/10.1016/0003-2697(87)90135-7
43. Sreerama N, Woody RW (1993) A Self-Consistent Method for the Analysis of Protein Secondary Structure from Circular Dichroism. Anal Biochem 209(1):32–44. https://doi.org/10.1006/abio.1993.1079
44. Provencher SW, Glöckner J (1981) Estimation of globular protein secondary structure from circular dichroism. Biochemistry 20:33–37. https://doi.org/10.1021/bi00504a006
45. Van Stokkum IHM, Spoelder HJ, Bloemendal M et al (1990) Estimation of protein secondary structure and error analysis from circular dichroism spectra. Anal Biochem 191:110–118
46. Sreerama N, Woody RW (2000) Estimation of protein secondary structure from circular dichroism spectra: Comparison of CONTIN, SELCON, and CDSSTR methods with an expanded reference set. Anal Biochem 287:252–260. https://doi.org/10.1006/abio.2000.4880
47. Micsonai A, Wien F, Bulyáki É et al (2018) BeStSel: A web server for accurate protein secondary structure prediction and fold recognition from the circular dichroism spectra. Nucleic Acids Res 46:315–322. https://doi.org/10.1093/nar/gky497
48. Moran NA, Jarvik T (2010) Lateral transfer of genes from fungi underlies carotenoid production in aphids. Science 328(5978):624–627. https://doi.org/10.1126/science.1187113
49. Horikawa M, Hashimoto T, Asakawa Y et al (2006) Uroleuconaphins A1 and B1, two red pigments from the aphid Uroleucon nigrotuberculatum (Olive). Tetrahedron 62:9072–9076. https://doi.org/10.1016/j.tet.2006.06.111
50. Ramasubbu N, Ragunath C, Mishra PJ (2003) Probing the role of a mobile loop in substrate binding and enzyme activity of human salivary amylase. J Mol Biol 325:1061–1076. https://doi.org/10.1016/S0022-2836(02)01326-8
51. Sumida M, Yamashita O (1977) Trehalase transformation in silkworm midgut during metamorphosis. J Comp Physiol B 115:241–253. https://doi.org/10.1007/BF00692534
52. Lee JH, Saito S, Mori H et al (2007) Molecular cloning of cDNA for trehalase from the european honeybee, Apis mellifera L., and its heterologous expression in Pichia pastoris. Biosci Biotechnol Biochem 71:2256–2265. https://doi.org/10.1271/bbb.70239
53. Sumida M, Ogura S, Miyata S et al (1989) Purification and some properties of trehalase from Chaetomium aureum MS-27. J Ferment Bioeng 67:83–86. https://doi.org/10.1016/0922-338X(89)90184-0
54. Shi ZK, Wang SG, Zhang T et al (2019) Three novel trehalase genes from Harmonia axyridis (Coleoptera: Coccinellidae): cloning and regulation in response to rapid cold and re-warming. 3 Biotech 9:321. https://doi.org/10.1007/s13205-019-1839-9
55. Shi Z, Liu X, Xu Q et al (2016) Two novel soluble trehalase genes cloned from Harmonia axyridis and regulation of the enzyme in a rapid changing temperature. Comp Biochem Physiol B Biochem Mol Biol 198:10–18. https://doi.org/10.1016/j.cbpb.2016.03.002
56. Tang B, Wei P, Zhao L et al (2016) Knockdown of five trehalase genes using RNA interference regulates the gene expression of the chitin biosynthesis pathway in Tribolium castaneum. BMC Biotechnol 16:1–14. https://doi.org/10.1186/s12896-016-0297-2
57. Yu HZ, Huang YL, Lu ZJ et al (2020) Inhibition of trehalase affects the trehalose and chitin metabolism pathways in Diaphorina citri (Hemiptera: Psyllidae). Insect Sci. https://doi.org/10.1111/1744-7917.12819
58. Zhao L, Yang M, Shen Q et al (2016) Functional characterization of three trehalase genes regulating the chitin metabolism pathway in rice brown planthopper using RNA interference. Sci Rep 6:1–14. https://doi.org/10.1038/srep27841
59. Nardelli A, Vecchi M, Mandrioli M, Manicardi GC (2019) The evolutionary history and functional divergence of trehalase (treh) genes in insects. Front Physiol 10:1–11. https://doi.org/10.3389/fphys.2019.00062